# Intelligent MagLev Slider System by Feedback of Gap Sensors to Suppress 5-DOF Vibration

Yi-Ming Kao, Nan-Chyuan Tsai*, Hsin-Lin Chiu

Department of Mechanical Engineering,
National Cheng Kung University
Tainan City 70101, Taiwan (ROC)
email: *nortren@mail.ncku.edu.tw

*Abstract*—This paper is focused at position deviation regulation upon a slider by Fuzzy Sliding Mode Control (FSMC). Five Degrees Of Freedom (DOFs) of position deviation are required to be regulated except for the direction (i.e., X-axis) in which the slider moves forward and backward. At first, the system dynamic model of slider, including load uncertainty and load position uncertainty, is established. Intensive computer simulations are undertaken to verify the validity of proposed control strategy. Finally, a prototype of realistic slider position deviation regulation system is successfully built up. According to the experiments by cooperation of pneumatic and magnetic control, the actual linear position deviations of slider can be regulated within (-40, +40)µm and angular position deviations within (-2, +2)mini-degrees. From the viewpoint of energy consumption, the applied currents to 8 sets of MAs are all below 1A. To sum up, the closed-loop levitation system by cooperation of pneumatic and magnetic control is capable to account for load uncertainty and uncertainty of the standing position of load to be carried.

*Keywords- Position Deviation Regulation; Fuzzy Sliding Mode Control (FSMC); Magnetic Levitation (MagLev).*

## I.    INTRODUCTION

In recent years, a few types of active non-contact slider systems were proposed. An air-driven slider was presented by Denkena *et al.* [1]. Based on their study, the compressed air not only can levitate the slider but also can drive the slider back and forth. Unlike pneumatic actuators, a 5-DOF (5 Degrees of Freedom) active magnetic levitation slider was reported by Kim *et al.* [2]. However, the applied currents to the magnetic actuators are up to 10A to counterbalance the weight of the slider.

In comparison to the air-driven actuator, in general the required force by magnetic actuator is relatively much larger. Hence, the bending phenomenon on thinner portion of slider would become easier to occur if the applied magnetic force exceeds over a certain level. Not only the heat dissipation problem has to be considered but also the electronic circuit of power amplifier is more complicated than the other low-power actuators. Among the available research reports regarding active levitation sliders, the most acceptable design by industries was proposed by Ro *et al.* [3]. In their work, four magnetic actuators are allocated at the corners of the slider to account for external disturbance. The weight of the slider and load is supported by the force component by air actuator. Additionally, a linear motor, to drive the slider

back and forth, is equipped at the middle of the guide rail. Nevertheless, there exists a common disadvantage: both uncertainties of load to be carried and the standing position of load during the loading/unloading process onto the slider are not counted into consideration of the corresponding control stratagy at all.

For high-precision machines and production, it often needs a slider system, which can account for load uncertainty and suppress undesired vibration effectively. However, no matter contact-type slider or aerostatic slider is employed, the slider systems are lack of the capability against load uncertainty and multi-degree-of-freedom vibration during the transportation of carried load. Therefore, an active robust slider levitation system is proposed by this paper to deal with the induced position deviation of the slider due to load uncertainty and load position uncertainty.

The rest of this article is organized as follows. In Section 2, the dynamic model of slider levitation system is developed. In Section 3, the fuzzy sliding mode control law is proposed. In Section 4, the experiments to examine the capability of the maglev slider to account for load uncertainty and uncertainty of the standing position are undertaken. Finally, conclusions are presented in Section 5.

## II.    DYNAMIC MODEL OF SLIDER LEVITATION SYSTEM

The mechanical structure of the proposed slider levitation system by cooperation of pneumatic and magnetic control is schematically shown in Fig. 1. In Fig. 1, "S" is the mass center of the slider. "S" is also the origin of the coordinate system. $\phi$, $\theta$ and $\psi$ are angular position deviations along X-axis, Y-axis and Z-axis respectively. y and z are the linear position deviations along Y-axis and Z-axis respectively. Eight sets of Magnetic Actuators (MAs) and an Electro-Pneumatic Transducer (EPT) are employed together to regulate both angular and linear position deviations of the slider. The four sets of magnetic actuators, Vertical Magnetic Actuators (VMAs), along with the EPT, are employed to together regulate the angular position deviations along X- and Y-axes and the linear position deviation along Z-axis. Another four sets of magnetic actuators, i.e., Horizontal Magnetic Actuators (HMAs), are employed to regulate the angular position deviation along Z-axis and position deviation along Y-axis. Three Vertical Gap Sensors (VGSs) are equipped to measure the linear position deviation along Z-axis. Besides, the angular

position deviations along X-axis and Y-axis can be estimated by the linear position deviations measured by these 3 VGSs at the same time. On the other hand, two Horizontal Gap Sensors (HGSs) are equipped to measure the linear position deviation along Y-axis. It is noted that the angular position deviation along Z-axis can be evaluated by the linear position deviations measured by the aforesaid HGSs.
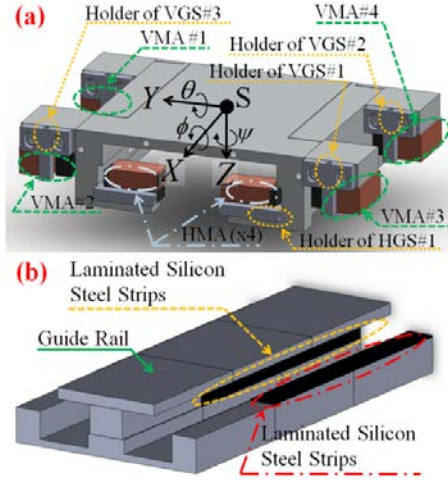


Figure 1. Schematic diagram of proposed levitation slider: (a) Slider, (b) Guide Rail.

The dynamic equations in terms of force/moment at equilibrium of the slider dynamics can be described as follows:

$$(m+\Delta m)\ddot{y} - \frac{A_u\mu_A}{g_u}\dot{y} = F_y^{MA} \tag{1a}$$

$$(m+\Delta m)\ddot{z} - A_s\mu_A(\frac{1}{g_l}+\frac{1}{g_r})\dot{z} = F_z^{MA} - F_a + \Delta mg \tag{1b}$$

$$(I_x+\Delta md_x^{\;2})\ddot{\phi} - A_s l_{sx}\mu_A(\frac{l_{sx}}{g_l}+\frac{l_{sx}}{g_r})\dot{\phi} = M_x^{MA} + \Delta mgd_x \tag{1c}$$

$$(I_y+\Delta md_y^{\;2})\ddot{\theta} - A_s\mu_A(\frac{\int_0^{l_{sy}}rdr}{g_l}+\frac{\int_0^{l_{sy}}rdr}{g_r})\dot{\theta} = M_y^{MA} + \Delta mgd_y \tag{1d}$$

$$(I_z+\Delta md_z^{\;2})\ddot{\psi} - A_u\mu_A\frac{\int_0^{l_{sy}}rdr}{g_u}\dot{\psi} = M_z^{MA} \tag{1e}$$

where $m$ is the mass of the slider, and $\Delta m$ the mass of load. $I_x$, $I_y$ and $I_z$ are the moments of inertia of the slider along X-axis, Y-axis and Z-axis respectively. $d_x$, $d_y$ and $d_z$ are the distances between the centroid of load and X-axis, Y-axis and Z-axis respectively. $A_u$ and $A_s$ are the area of the upper surface and side surface of guide rail respetively. $\mu_A$ is viscosity coefficient of air. $l_{sx}$ is the distance between the inner-side wall of slider and X-axis, $l_{sy}$ the distance between Y-axis and the front/tail of slider. $g_u$, $g_l$ and $g_r$ are the air gaps between the slider and guide rail on the upper side, left

side and right side of guide rail respectively. $\tau_{\phi l}$ and $\tau_{\phi r}$ are the shear stresses induced by the air on the inner wall of slider as the slider rotates along X-axis. In similar fashion, $\tau_{\theta r}$ and $\tau_{\theta l}$ are the shear stresses induced by the air on the inner wall of slider as the slider rotates along Y-axis. By same arguments, $\tau_{\psi}$ is the shear stress induced by the air on the inner wall of slider as the slider rotates along Z-axis. As long as the velocity component along +Z-axis of slider is present, two types of shear stresses, i.e., $\tau_{zl}$ and $\tau_{zr}$ are generated. Likewise, the shear stress $\tau_y$ emerges as long as the velocity component along +Y-axis of slider is not zero. $M_x^{MA}$, $M_y^{MA}$ and $M_z^{MA}$ are the moments induced by magnetic actuators along X-axis, Y-axis and Z-axis respectively. $F_y^{MA}$, $F_z^{MA}$ and $F_a$ are the resultant force by HMAs, the resultant force by VMAs and the applied force by EPT respectively.

## III. FUZZY SLIDING MODE CONTROL

For a slider, in general the mass of carried load and the standing location of the load are not fixed all the time. This implies that a certain degree of uncertainties is embedded in the dynamic model of the slider system. Therefore, the basic concept of Sliding Mode Control (SMC) [4]-[6] is adopted by our work. Moreover, fuzzy logic [7]-[11] is additionally applied to adjust slope of the corresponding sliding surface, based on the real-time trajectory tracking error and error rate, such that superior system response can be achieved. That is, FSMC (Fuzzy Sliding Mode Control) is proposed to replace the standard SMC by this research.

### A. Design of Controller

Before FSMC is synthesized, the dynamic equations of the slider system, i.e., (1), are deduced into another form to aim at uncertainties of load and load position:

$$\ddot{q} = f + u \tag{2}$$

where

$$q=[y \quad z \quad \phi \quad \theta \quad \psi]^T \tag{3a}$$

$$f = \begin{bmatrix} \dfrac{A_u\mu_A\dot{y}}{(m+\Delta m)g_u} \\[4pt] \dfrac{A_s\mu_A\dot{z}}{m+\Delta m}(\dfrac{1}{g_l}+\dfrac{1}{g_r})+\dfrac{\Delta mg}{m+\Delta m} \\[4pt] \dfrac{A_s\mu_A l_{sx}^{\;2}\dot{\phi}}{I_x+\Delta md_x^{\;2}}(\dfrac{1}{g_l}+\dfrac{1}{g_r})+\dfrac{\Delta mgd_x}{I_x+\Delta md_x^{\;2}} \\[4pt] \dfrac{A_s\mu_A\int_0^{l_{sy}}rdr}{I_y+\Delta md_y^{\;2}}(\dfrac{1}{g_l}+\dfrac{1}{g_r})+\dfrac{\Delta mgd_y}{I_y+\Delta md_y^{\;2}} \\[4pt] \dfrac{A_u\mu_A\int_0^{l_{sz}}rdr}{(I_z+\Delta md_z^{\;2})g_u}\dot{\psi} \end{bmatrix} \tag{3b}$$

$$u = \begin{bmatrix} \dfrac{F_y^{MA}}{m+\Delta m} & \dfrac{F_z^{MA}-F_a}{m+\Delta m} & \dfrac{M_x^{MA}}{I_x+\Delta m d_x^2} & \dfrac{M_y^{MA}}{I_y+\Delta m d_y^2} & \dfrac{M_z^{MA}}{I_z+\Delta m d_z^2} \end{bmatrix}^T \quad (3c)$$

Since the mass of load and the standing location of load are not fixed all the time, $d_x$, $d_y$, $d_z$ and $\Delta m$ are all variables in this system. For the uncertain system dynamics, its nominal model, $f_0$, is defined as follows:

$$f_0 = \begin{bmatrix} \dfrac{A_u \mu_A}{m \cdot g_u} \dot{y} \\[2ex] \dfrac{A_s \mu_A}{m}(\dfrac{1}{g_l}+\dfrac{1}{g_r})\dot{z} \\[2ex] \dfrac{A_s \mu_A l_{sx}^2}{I_x}(\dfrac{1}{g_l}+\dfrac{1}{g_r})\dot{\phi} \\[2ex] \dfrac{A_s \mu_A \int_0^{l_{sy}} r\,dr}{I_y}(\dfrac{1}{g_l}+\dfrac{1}{g_r})\dot{\theta} \\[2ex] \dfrac{A_u \mu_A \int_0^{l_{sz}} r\,dr}{I_z g_u}\dot{\psi} \end{bmatrix} \quad (4)$$

Consequently, the system uncertainty, $f - f_0$, is assumed to be bounded by a functional, $W^{smc}$:

$$\left| f - f_0 \right| \leq W^{smc} \quad (5)$$

The sliding functional, $S$, can be defined as follows:

$$S = \lambda e + \dot{e} = \lambda(q_r - q) + (\dot{q}_r - \dot{q}) \quad (6)$$

where $e$ represents the vector of differences between the actual state and the desired state, $q$ the actual state vector, $q_r$ the vector of desired state trajectory, $\lambda$ the slope of phase plot of the state tracking error and its error rate. In order to ensure the system remains on the sliding surface, the sliding condition, i.e., $S = 0$, has to be imposed. Based on the sliding condition [4]-[6] and (2), the equivalent control component can be obtained:

$$u_{eq} = -f_0 + \ddot{q}_r + \lambda \dot{e} \quad (7)$$

On the other hand, to satisfy the reaching condition, i.e., $S\dot{S} < 0$, the switching control component can be designed as follows:

$$u_{sw} = -K^{smc} \cdot Sgn(S) \quad (8)$$

where $K^{smc}$ is a positive definite matrix and " $Sgn$ " represents the symbol operator. Explicitly, $K^{smc}$ and $Sgn$ are defined as follows:

$$K^{smc} = diag(K_1^{smc} \ K_2^{smc} \ K_3^{smc} \ K_4^{smc} \ K_5^{smc}) \quad (9a)$$

$$Sgn(S) = \begin{cases} 1 & if \ \ S > 0 \\ 0 & if \ \ S = 0 \\ -1 & if \ \ S < 0 \end{cases} \quad (9b)$$

where the parameters $K_1^{smc} \sim K_5^{smc}$ are named as reaching factors. They can dominate the reaching speed of the deviated state, off the sliding surface, approaching towards the sliding surface. Finally, the composite control input by SMC policy, $u$, is added up as follows:

$$u = u_{eq} + u_{sw} \quad (10)$$

As usual, the Lyapunov direct method is employed to examine the stability for the proposed control policy. The Lyapunov candidate is defined as follows:

$$V = \frac{1}{2} S^T S > 0, \text{ where } \forall S \neq 0 \quad (11)$$

The derivative of Lyapunov candidate can be obtained as follows:

$$\dot{V} = (f - f_0)S - K^{smc}\left|S\right| \leq (W^{mc} - K^{smc})\left|S\right| \equiv -\eta\left|S\right| \quad (12)$$

To satisfy (12), $K^{smc}$ can be chosen as follows:

$$K^{smc} = W^{smc} + \eta \quad (13)$$

By substituting (13) into (8), the composite control, $u$, can be described as follows:

$$u = u_{eq} - [W^{smc} + \eta]Sgn(S) \quad (14)$$

By adding FLA (Fuzzy Logic Algorithm) to adjust the slope of the sliding surface is the main concept to adopt FSMC, instead of standard SMC alone. The schematic configuration of the closed-loop slider system is shown in Fig. 2. The transformation matrix $\alpha$ is utilized to convert the measurements from the 5 sets of gap sensors into the form of changes of state variables. The slope of the sliding surface, $\lambda_i$, $i = y$, $z$, $\phi$, $\theta$ or $\psi$, is adaptively altered by the real-time fuzzy algorithm based on state tracking error and rate of state tracking error. The transformation matrix $\beta$ is employed to convert the controller outputs into the required control current/voltage with respect to the corresponding actuators.
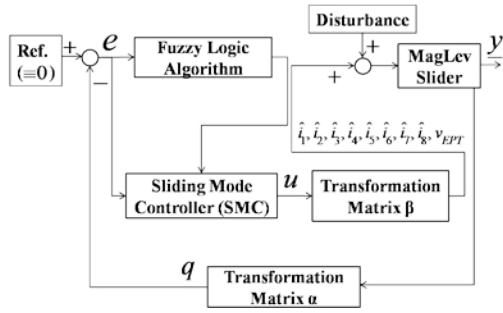
Figure 2.  Schematic configuration of closed-loop slider system under FSMC.

The interested rules of FLA are summarized and listed in Table 1. $e_i$, $\dot{e}_i$ and $c_i$ are the state tracking error, rate of the state tracking error and the output of FLA respectively. Seven fuzzy sets with triangle membership functions (NB, NM, NS, ZE, PS, PM, PB) are set for $e_i$, $\dot{e}_i$ and $c_i$. The subscript, $i$, denotes $y$, $z$, $\phi$, $\theta$ or $\psi$. $\mu(e_i)$, $\mu(\dot{e}_i)$ and $\mu(c_i)$ are the corresponding membership functions of $e_i$, $\dot{e}_i$ and $c_i$. Finally, by using the method based on Center Average Defuzzification (CAD)[12], the corresponding output of FSMC, $u_{crisp}$, can be obtained by the defuzzification interface. The crisp control command can be evaluated as follows:

$$u_{crisp} = [\,\mu_{PB}(c_i)\cdot 1 + \mu_{PM}(c_i)\cdot(2/3) + \mu_{PS}(c_i)\cdot(1/3) + \mu_{NS}(c_i)\cdot(-1/3) \quad (15)$$
$$+ \mu_{NM}(c_i)\cdot(-2/3) + \mu_{NB}(c_i)\cdot(-1)] / [\mu_{PB}(c_i) + \mu_{PM}(c_i) + \mu_{PS}(c_i)$$
$$+ \mu_{ZE}(c_i) + \mu_{NS}(c_i) + \mu_{NM}(c_i) + \mu_{NB}(c_i)]$$

TABLE I.  RULE BASE FOR FLA



|  | NB | NM | NS | ZE | PS | PM | PB |
|---|---|---|---|---|---|---|---|
| NB | NB | NB | NB | NB | NM | NS | ZE |
| NM | NB | NB | NB | NM | NS | ZE | PS |
| NS | NB | NB | NM | NS | ZE | PS | PM |
| ZE | NB | NM | NS | ZE | PS | PM | PB |
| PS | NM | NS | ZE | PS | PM | PB | PB |
| PM | NS | ZE | PS | PM | PB | PB | PB |
| PB | ZE | PS | PM | PB | PB | PB | PB |

NB  Negative Big
NM  Negative Medium
NS  Negative Small
ZE  Zero
PS  Positive Small
PM  Positive Medium
PB  Positive Big

### B.  Computer Simulations

At the stage of computer simulations, two cases are to be studied:
Caes I: Load (1kg) added onto slider
Case II: Load (1kg) subtracted out of slider

#### 1)  Load added onto slider (Case I)

An additional load of 1 kg, is put onto the slider at the position, $(x, y, z) = (5\,cm, 5\,cm, 0)$ at $Time = 2s$, for **Case I**. However, the mass center of the slider is at $(x, y) = (0, 0)$. Since the load is not put onto the position of mass center of the slider, the angular position deviations are hence induced. The corresponding computer simulations are shown in Fig. 3(a).  It is observed that an outstanding linear position deviation along +Z-axis occurs at $Time = 2s$.  Besides, most often the load is not exactly thrown at the position of mass center of the slider, the angular position deviations along X-axis and Y-axis are hence induced as the load is added onto the slider.  In similar fashion, the applied currents to VMA#1~VMA#4 are all increased to account for the angular position deviations along X-axis and Y-axis.
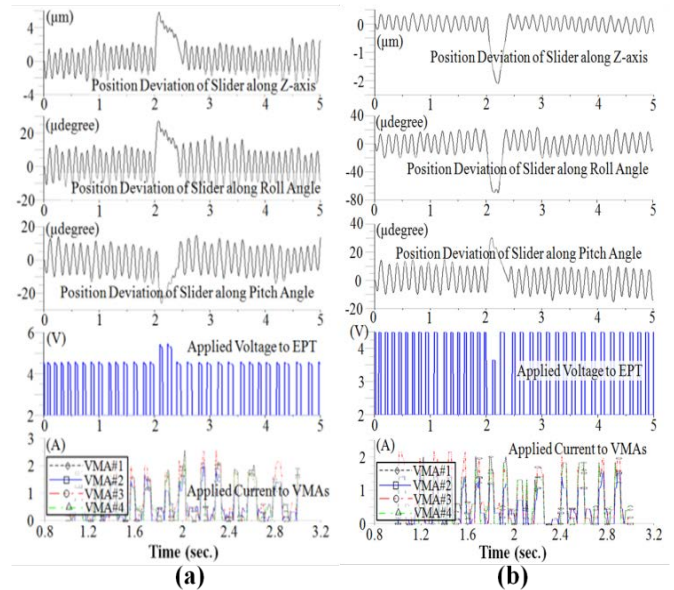


Figure 3.  Position deviations regulation on slider: (a) load added onto slider at position $(x, y, z) = (5\,cm, 5\,cm, 0)$, (b) load subtracted at position $(x, y, z) = (5\,cm, 5\,cm, 0)$.

#### 2)  Load subtracted out of slider (Case II)

A carried load, with weight quantity 1kg, is subtracted out of the slider at position $(x, y, z) = (5\,cm, 5\,cm, 0)$ at $Time = 2s$, for **Case II**.  The corresponding computer simulations are shown in Fig. 3(b).  Accordingly, an outstanding linear position deviation along –Z-axis is induced at the same time.  In addition, the currents applied at VMA#1~VMA#4 are all reduced but still have to cooperate with EPT.  On the other hand, since the load subtracted is hardly located exactly at the position of mass center of the slider, the corresponding currents applied at VMA#1~VMA#4, to suppress the angular position deviations along X-axis and Y-axis, are usually necessary.

### IV.  EXPERIMENTAL VERIFICATION

The photograph of proposed MagLev slider system by cooperation of pneumatic and magnetic actuators is shown in Fig. 4.  A set of pneumatic cylinder and air pump is

equipped to generate the power to move the slider forwards and backwards along X-axis. The schematic diagram of the experimental setup is shown in Fig. 5. Two categories of experiments are to be undertaken, namely, *PART I* and *PART II*. For *PART I*, an additional load, with weight 1kg, is added onto the slider at $(x, y, z) = (5\,cm, 5\,cm, 0)$ at $Time = 0.1s$. The aforesaid additional load is later-on substracted out of the slider for *PART II*.
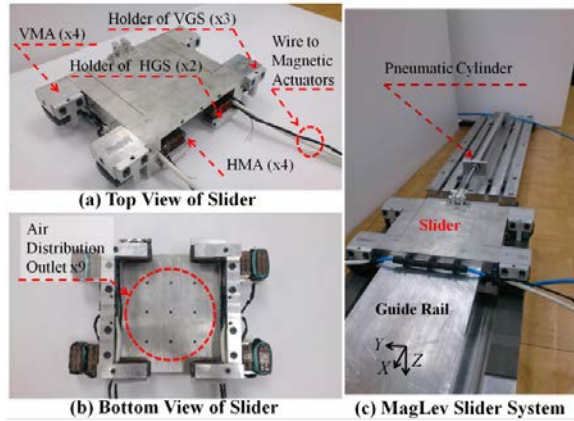


Figure 4.   Photograph of MagLev slider system
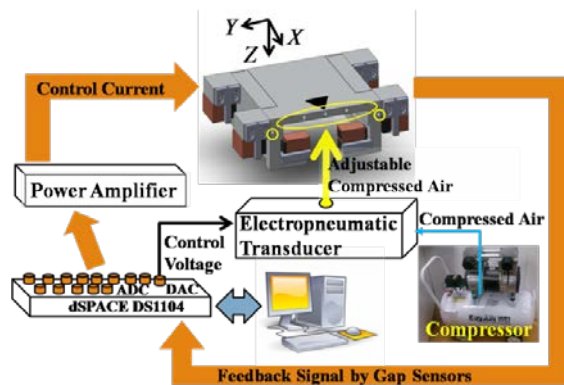


Figure 5.   Schematic diagram of experimental setup

## A.   PART I: Additional Load Added

An additional load, with weight 1kg, is put onto the slider at position $(x, y, z) = (5\,cm, 5\,cm, 0)$ at $Time = 0.1s$. It is noted that the mass center of the slider on the horizontal plane is at $(x, y) = (0, 0)$. Obviously, the standing location of the added load does not coincide with the mass center of the slider so that outstanding angular position deviations due to this applied moment by load weight are hence induced. The experimental results for position deviation regulation on slider in 5 DOF are shown in Fig. 6. The maximum linear position deviations along Z-axis and Y-axis induced by the additional load are 80μm and 130μm respectively. The linear position deviations along Z-axis and Y-axis can be suppressed to $\pm$ 20μm and $\pm$ 40μm respectively within 0.1sec. In addition, the maximum angular position deviations along X-axis, Y-axis and Z-axis are $4.5 \times 10^{-3}$ degree, $-3 \times 10^{-3}$ degree and $5 \times 10^{-3}$ degree

respectively. The angular position deviations along X-axis, Y-axis and Z-axis can be all regulated within $\pm 2 \times 10^{-3}$ degree in 0.1sec. It is concluded that both of the linear position deviations and angular position deviations can be completely suppressed within a very short time interval (about 0.1sec). On the other hand, the applied currents to the magnetic actuators, shown in Fig. 7, are jointly adjusted accordingly so that the induced tilt about X-axis and the induced pitch about Y-axis can be suppressed. Since most of the weight of the slider and load is supported by the supportive force by the high pressurized air, the applied currents to VMAs are not increased much to counterbalance the weight of the additional load newly put on. It is observed that the average applied currents to VMAs are all below 0.2A. The applied currents to VMAs in the undertaken experiments are much lower than that in computer simulations stated in previous section. The reason might be stemmed from the actual viscosity and friction in vertical direction being more serious in real world but neglected in computer simulations under over-simplified assumptions for interconnection between any two components in motion.
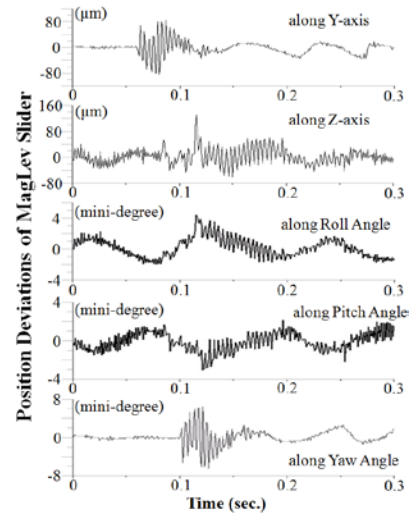


Figure 6.   Position deviations regulation on slider by experiments (*Part I*)
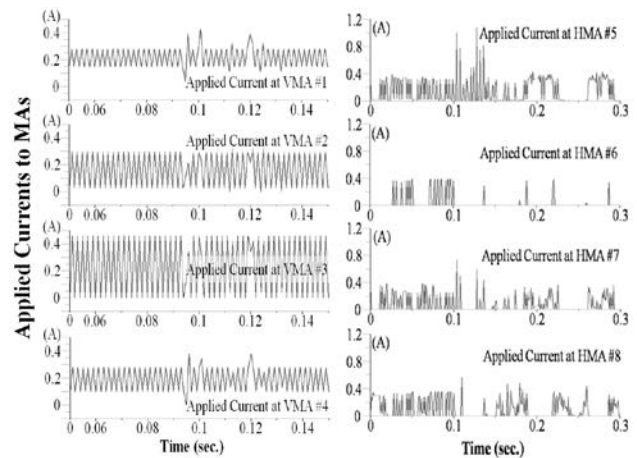


Figure 7.   Applied currents at MAs by experiments (*Part I*)

## B. Part II: Partial Load Subtracted

A partial load, with weight 1kg, is subtracted out of the slider at position $(x, y, z) = (5\,cm, 5\,cm, 0)$ at $Time = 0.05s$. The experimental results for position deviations regulation on slider in 5 DOF are shown in Fig. 8. The position deviations along 5-axes can be completely suppressed within a very short time interval (about 0.15sec). In similar fashion, the applied currents to the magnetic actuators, shown in Fig. 9, are jointly adjusted as well to regulate the induced tilt and pitch motions. Since partial load is taken off the slider, the average applied currents to VMAs become only half of those in *Part I*. Besides, the maximum applied currents to HMAs are all below 0.5A. Nevertheless, the currents applied to VMAs and HMAs are still required and absolutely necessary in order to counterbalance the external disturbance, particularly for the transient time period as the partial load suddenly removed, no matter how significantly the quantities of consumed electricity at magnetic actuators are reduced.
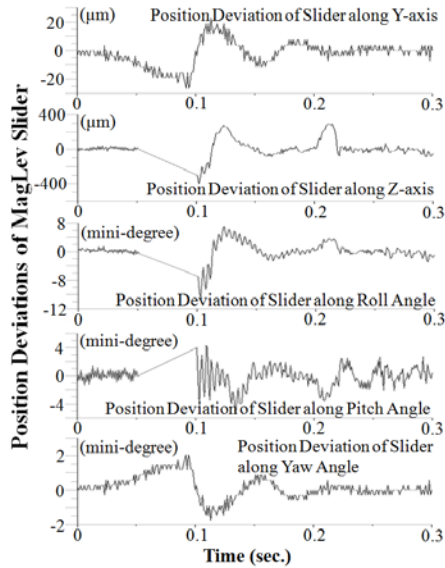


Figure 8.   Position deviations regulation on slider by experiments (*Part II*).
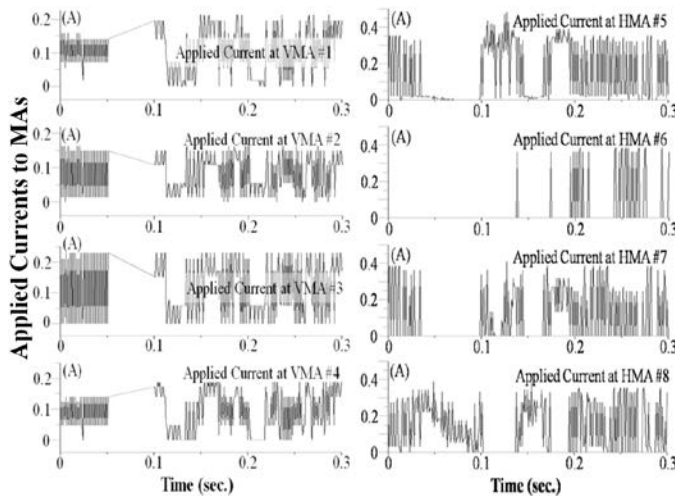


Figure 9.   Applied currents at MAs by experiments (*Part II*)

## V.   CONCLUSION

An active robust MagLev slider system is proposed to deal with the induced position deviations of the slider due to load uncertainties and load position uncertainties. By cooperation of pneumatic and magnetic actuators, efficient regulations of the position deviations of slider in 5 DOF can be achieved. According to the experiments undertaken, the actual linear position deviations of slider can be regulated within $\pm$ 40μm and angular position deviations within $\pm$ 2mini-degrees. Besides, the applied currents to the 8 sets of MAs are all below 1A. The closed-loop slider levitation system is fairly capable to account for load uncertainties and load position uncertainties. To sum up, by the cooperation of pneumatic and magnetic actuators, the proposed closed-loop slider system exhibits the merits of stabilization to the inherently unstable system, capability for simultaneous position regulation in 5 DOF and outstanding reduction of energy consumption.

## REFERENCES

[1]   C. H. Kim, K. J. Kim, J. S. Yu, and H. W. Cho, "Dynamic Performance Evaluation of 5-DOF Magnetic Levitation and Guidance Device by Using Equivalent Magnetic Circuit Model", *IEEE Transactions on Magnetics*, vol. 49, no. 7, pp. 4156-4159, 2013.

[2]   B. Denkena, H. C. Möhring, and H. Kayapinar, "A novel fluid-dynamic drive principle for desktop machines", *CIRP Journal of Manufacturing Science and Technology*, vol. 6, no. 2, pp. 89-97, 2013.

[3]   S. K. Ro, S. Kim, Y. Kwak, and C. H. Park, "A linear air bearing stage with active magnetic preloads for ultraprecise straight motion", *Precision Engineering*, vol. 34, no. 1, pp. 186-194, 2010.

[4]   W. Perruquetti and J. P. Barbot, Sliding Mode Control in Engineering. New York, NY: Marcel Dekker. 2002.

[5]   V. I. Utkin and V. Ivanovich, Sliding Mode Control in Electromechanical Systems, London: Taylor&Francis, 1999.

[6]   Y. Shtessel, Sliding Mode Control and Observation, Birkhäuser, New York:Control Engineering, 2014.

[7]   M. Jamshidi, N. Vadiee, and T. J. Ross, "Fuzzy logic and control : software and hardware applications", 1993.

[8]   D. Driankov, "An Introduction to Fuzzy Control," 1996.

[9]   C. C. Lee, "Fuzzy Logic in Control Systems: Fuzzy Logic Controller-Part I, II", *IEEE Transactions on Systems, Man, and Cybernetics: Systems includes the fields of systems engineering*, vol. 20, issue 2, pp. 404-435, 1990.

[10]  N. F. Al-Muthairi and M. Zribi, "Sliding Mode Control of a Magnetic Levitation System", *Mathematical Problems in Engineering*, vol. 2, pp. 93-107, 2004.

[11]  A. K. Ahmad, Z. Saad, M. K. Osman and S. K. Abdullah, "Control of Magnetic Levitation System Using Fuzzy Logic Control", *Second International Conference on Computational Intelligence, Modelling and Simulation*, 2010.

[12]  K. M. Passino and S. Yurkovich, "Fuzzy Control," Addison Wesley, 1998.